Planning and Operation of Isolated Microgrids Based on Repurposed Electric Vehicle Batteries

Talal Alharbi [ID], *Student Member, IEEE*, Kankar Bhattacharya [ID], *Fellow, IEEE*, and Mehrdad Kazerani, *Senior Member, IEEE*

Abstract—Battery energy storage systems (BESSs) can be very beneficial to power systems and microgrids for various applications. With increasing sales of electric vehicles (EV), the availability of used electric vehicle batteries (EVBs) is on the rise, which has received significant attention in recent years. The retired EVBs, after repurposing, can serve as an alternative option to new batteries in a BESS. In addition, when a microgrid operator desires to install a BESS, the optimal decisions such as installation year, energy and power size, replacement year, and the number of cycles to failure, that are normally overlooked, have to be determined. Therefore, this paper proposes a comprehensive and novel framework for planning and operation of the BESS based on repurposed EVBs. A novel linearized BESS sizing model is proposed that obtains the BESS optimal decisions regarding design and operation. Various new, modified, and linearized relationships for the BESS have been included in the planning model to ensure that the replacement year of the BESS is optimally determined. Several classes of EVs with multiple drive cycles are clustered and integrated within the proposed framework.

Index Terms—Degradation, isolated microgrid, optimal planning, repurposed electric vehicle battery (REVB).

NOMENCLATURE

A. Indices

i	Index for generating units, $i = 1, ..., G$.
t	Index for operation steps, $t = 1, ..., T$ [hour].
y	Index for planning steps, $y = 1, ..., N$ [year].

B. Parameters

C^{UNS}	Cost of unserved demand [\$/kWh].
C_E^v, C_{pb}^v	BESS variable installation costs of energy and power capacities, respectively [\$/kWh, \$/kW].
C^{fx}	Fixed installation cost of the REVB and new BESS [\$].
OMC^{fx}	Fixed O&M cost of the REVB and new BESS [\$/kW].
OMC^v	Variable O&M cost of the REVB and new BESS [\$/kW].
$Pd_{y,t}$	Isolated microgrid demand at hour t, year y [kW].
$P_{y,t}^{\mathrm{PV}}$	Solar power output forecast at hour t, year y [kW].
$P_{y,t}^W$	Wind power output forecast at hour t, year y [kW].
RC	Replacement cost [\$/kWh].
M	Large number.
$\eta_{\mathrm{ch}}, \eta_{\mathrm{dch}}$	BESS charging and discharging efficiency, respectively [%].

C. Decision Variables

AC_y	BESS added capacity at replacement year [kWh] .
B_y	BESS installation decision variable [1 or 0] .
CRB_y	BESS remaining energy capacity with respect to 80% of the rated capacity [kWh] [+, 0 , −].
CRB_y^+	CRB_y value when it is positive only [kWh].
CRB_y^-	CRB_y value when it is negative or zero [kWh].
CF_y^+	Binary variable when CRB_y value is positive.
CF_y^-	Binary variable when CRB_y value is negative.
E_y^{ini}	Initial energy capacity of BESS at installation [kWh].
$\underline{E_y}$	Minimum BESS capacity [kWh].
$\overline{E_y}$	Current BESS energy capacity [kWh].
$Edeg_y^{Cyc}$	Capacity degradation due to cycling effect [kWh].
$Edeg_y^{Cal}$	Capacity degradation due to calendar effect [kWh].
LC_y	BESS capacity loss due to degradation [kWh].
LRY_y	Bilinear variable used to replace the product of two variables, year of BESS replacement and initial BESS capacity [kWh].
$P_{y,t}^{\mathrm{UNS}}$	Unserved demand at time t and year y [kW].
$Pba_{y,t}$	BESS charging (−)/ discharging (+) power [kW].
$P_{i,y,t}$	Power output of generator i at hour t and year y [kW].
$P_{y,t}^{\mathrm{Res}}$	Reserved demand at hour t and year y [kW].
Pb_y^{ini}	Initial installation of BESS power rating [kW].
Pb_y	Current BESS power rating [kW].
RY_y^v	Replacement year [year].
$SOC_{y,t}$	SoC of the battery at hour t and year y [kWh].
$SRB_{y,t}$	Reserve provided to the system by the BESS [kW].
TED	Total discharged energy by the BESS in one day [kWh].

$U_{y,i,t}$	Start-up binary decision variable [1 or 0].
$V_{y,i,t}$,	Shut-down binary decision variable [1 or 0].
$W_{y,i,t}$	Unit-commitment binary decision variable [1: generation i is online, 0: otherwise].
$X_{y,t}^{\text{ch/dch}}$	Binary variable [1: BESS is charging or discharging, 0: otherwise].
Z_y^{RY}	BESS replacement year binary decision variable.
ζ	Total capacity loss due to cycling degradation of the EVB in Stage I.

I. INTRODUCTION

THE increasing penetration of electric vehicles (EVs) raises concerns of stockpiling of used electric vehicle batteries (EVBs) after their vehicular end of life (EoL) [1], [2]. Utilization of used EVBs, after repurposing, can play a significant role in isolated microgrids in alleviating the need for costly new battery energy storage systems (BESSs) or diesel generators in the long term, which is beneficial both economically and environmentally. Used and repurposed EVBs (REVBs) offer a viable option for small-scale or bulk deployment as BESSs, or as community energy storage systems. Researchers are examining various usages of REVBs in stationary applications, but only a few projects have been reported so far [3], [4]. To integrate REVBs in such applications, their capacity degradation and state of health (SoH) at the EoL need be considered. In [5], capacity degradation of Li-ion EVBs under different stress factors, such as temperature and state of charge (SoC) was determined; however, only the cycling effect was accounted for, and the calendar degradation effect was not considered.

For installation of new BESSs or REVBs in isolated microgrids, the following issues need to be considered:
1) determining the optimal year of installation, along with the optimal power and energy capacity ratings;
2) optimal operation of these devices;
3) proper consideration of calendar and cycling degradation of BESSs and REBVs;
4) determining an optimal year of BESS replacement, considering degradation, instead of using a fixed replacement year, which can lead to premature replacements and additional costs.

While the high investment cost associated with new BESSs can make them economically unattractive for microgrids, REVBs can provide the same services at a fraction of the cost of a new BESS [3]. Also, repurposing an EVB would delay its recycling and prolong its useful life.

In [6], sizing of the BESS was proposed using a two-stage optimization model considering various operational and planning constraints; however, the work did not consider battery degradation over the ten-year planning horizon. In [7], BESS planning in microgrids was carried out considering life-cycle degradation, by accounting for the number of cycles-to-failure (C2F); however, the reduction in BESS energy capacity due to cycling and calendar degradation was not considered. In [8], a stochastic optimization framework for BESS planning for isolated microgrids was proposed, wherein BESS cycling degradation was considered on a flat-rate basis, not capturing the true capacity loss during discharging, thus over- or underestimating energy capacity.

It should be noted that none of the above works attempted to determine the optimal year of BESS replacement. In [8], a fixed replacement year was considered, leading to premature replacement decisions and hence increasing the plan cost. Moreover, in most of the reported works, either the number of C2F or the impact of cycling and calendar degradations on the size is considered, but not both, which is necessary to accurately capture the BESS energy capacity and optimal operation. Also, there is a need to connect the stages of EVB life to test the viability of REVBs in secondary applications.

Therefore, the main objectives of this work are as follows:
1) Develop a systematic procedure to model the degradation of EVBs for different classes of EVs during their first-life in vehicles, and hence, incorporate these characteristics to estimate the expected cost of installing REVBs.
2) Develop a generic microgrid planning model to determine the optimal energy size, power rating, and optimal year of replacement of new BESSs and REVBs. The model needs to include the impact of degradation due to calendar and cycling effects on the BESS/REVBs' energy capacity, as well as on the number of C2F. The proposed model will introduce a novel set of mathematical relations for BESS degradation and optimal year of replacement, thereby avoiding premature replacements and additional costs.
3) Consider multiple drive cycles of different classes of EVs to capture their impact on the expected SoH of the EVBs and hence on the number of years until they reach their EoL. This leads to developing an expected degradation model of EVBs for each class, for inclusion in the generic microgrid planning model proposed earlier, to study the impact of uncertainties.

Based on the proposed work, following are the main envisaged contributions of the work presented in this paper:
1) The degradation characteristics and the SoH of EVBs are being captured and modeled in detail, considering cycling and calendar degradation using real EV drive cycle data.
2) A novel microgrid planning model is proposed that determines the optimal decisions on new BESSs or REVBs and the corresponding sizing and year of installation taking into account a new set of mathematical relations of BESS degradation and optimal year of replacement. The REVBs are modeled considering their first-life drive cycles and degradation, which impacts the microgrid planning decisions.
3) In order to capture the heterogeneity of EVBs and the impact of uncertainty in the planning model, multiple drive cycles of different classes of EV are used to develop a novel expected degradation model of EVB classes for inclusion in the microgrid planning model.

The structure of this paper is as follows: Section II describes the proposed framework, as well as the detailed mathematical models of each stage. In Section III, the proposed framework is simulated, and the results are presented to demonstrate the effectiveness of the proposed models with the exploration of various scenarios. Section IV presents a discussion of the algorithms used and computational aspects. Finally, conclusions are drawn in Section V.
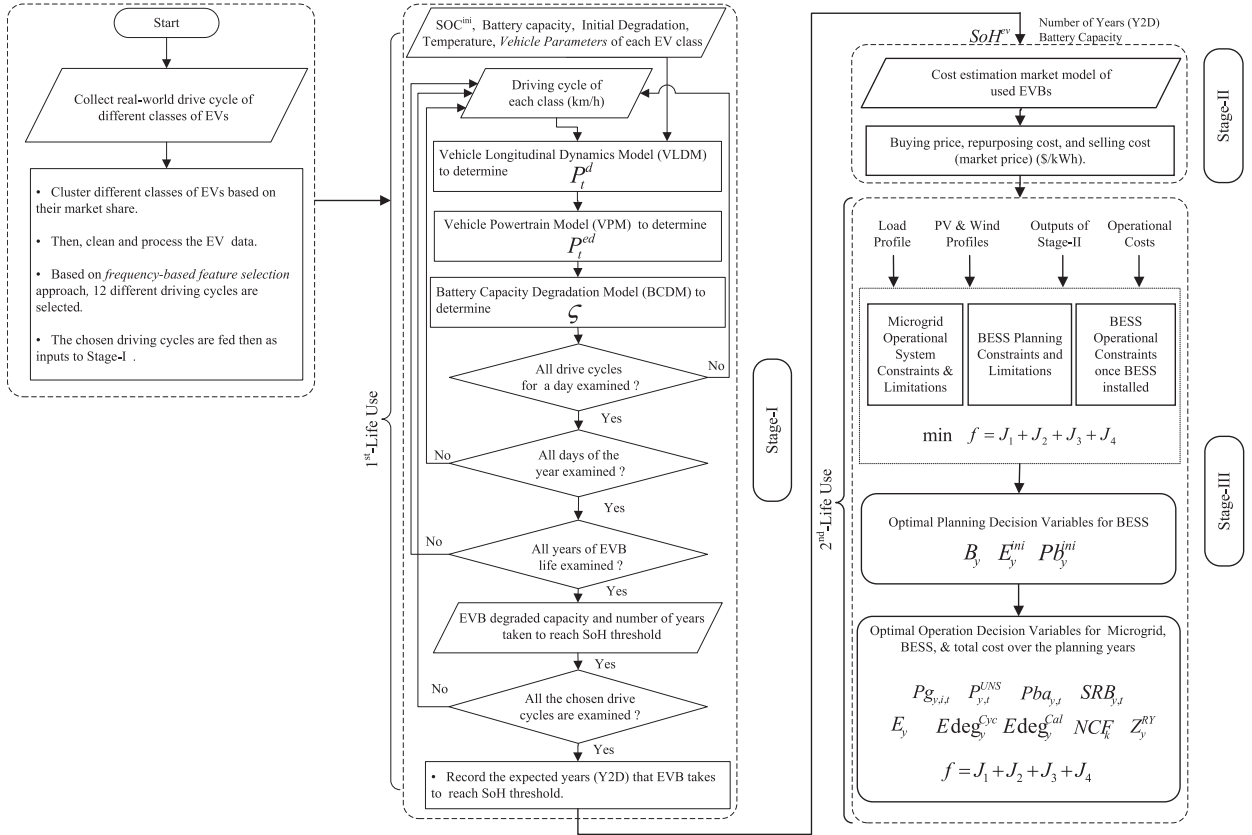
Fig. 1. Flowchart of the proposed systematic framework of REVB utilization.

II. PROPOSED MICROGRID PLANNING FRAMEWORK AND MATHEMATICAL MODELS

In this section, a novel schematic framework is proposed for modeling of EVBs during their first-use and subsequently their utilization as BESS in isolated microgrids for various second-use applications. The framework comprises three stages, presented in Fig. 1, which are discussed in detail in the following subsections; the important inputs to, and outputs from, each stage are clearly identified in the figure, and all assumptions are stated.

A. Stage I: EVB Capacity Degradation During Vehicular Life

A comprehensive flowchart of Stage I is shown in Fig. 1. This stage simulates the performance of an EVB during its first-life in an EV and determines its SoH at any instant, and the number of years it takes for the battery to degrade to its SoH threshold [9], considering cycling and calendar degradations. There is a need for real and detailed drive cycle data of different EV classes to accurately estimate the outputs.

This stage includes the following three models (see Fig. 1):
1) vehicle longitudinal dynamic model (VLDM) [10];
2) vehicle power-train model (VPM) [10];
3) battery capacity degradation model (BCDM) [5].

The simulation starts with reading all the parameters as inputs, which are then fed, together with the EV drive cycle, to the VLDM to calculate the mechanical traction power P_t^d. This power is transferred to the VPM to determine the electrical traction power demand, P_t^{ed}, needed from the battery. From P_t^{ed}, the SoC and temperature of the battery are calculated using the electrical and thermal models of the EVB, as explained in [11]; the EVB's capacity degradation and the SoH are determined from the BCDM [5]. However, it should be noted that [5] only accounts for degradation due to cycling (α_t^{Cyc}), while this paper, besides cycling degradation, considers a linear calendar degradation rate (α_t^{Cal}) as well. The initial SoC is 90%, and the EVB is recharged to 90% at the end of each drive cycle.

In this work, lithium iron phosphate (LiFePO$_4$)-based EVBs are considered; the BCDM of LiFePO$_4$ EVBs is expressed as a function of different stress factors, as follows:

$$\zeta(T, SoC_{\text{avg}}^{\text{ev}}, SoC_{\text{dev}}^{\text{ev}}) = \alpha_t^{\text{Cyc}} + \alpha_t^{\text{Cal}} \qquad (1)$$

where ζ is the total capacity loss due to cycling degradation of the EVB pack (α_t^{Cyc}), while α_t^{Cal} is calendar degradation of the EVB battery pack. The total capacity loss depends on the EVB temperature T and the average value and standard deviation of SoC, SoC_{avg}^{ev} and SoC_{dev}^{ev}, respectively. It should be noted that the inputs to the BCDM are results of EVB simulation based on a given drive cycle. The SoH of the EVB is calculated as follows [5]:

$$\text{SoH} = \left(1 - \frac{\zeta}{\text{Rated EVB Capacity}}\right). \qquad (2)$$

Stage I provides two main outputs that will have an impact on Stages II and III, the SoH, and the number of years it takes to degrade to 80% SoH threshold. The latter determines how many years REVB will stay in second-life applications (microgrid applications).

B. Stage II: Post Vehicular Life Assessment and Cost Estimation

Adopting the economic model from [12], the outputs of Stage I (e.g., SoH and number of years) are used to estimate the cost of an REVB, which includes the monetary value of the used EVB and the cost of repurposing; this is used to determine the economic feasibility of the REVB as compared to a new BESS in the long term. The cost of an REVB is dependent on module properties, cell fault rates, the used battery SoH, and initial and degraded capacities of the EVB.

C. Stage III: Microgrid Planning Model

The proposed planning model for isolated microgrids determines the optimal power rating and energy capacity of BESS, as well as optimal year of installation and replacement, taking into account the inherent cycling and calendar degradations. Accounting for degradation ensures realistic operational decisions and an optimal replacement year, thereby avoiding premature replacements and additional costs. Two different options for BESS are considered, i.e., REVBs and new BESSs.

1) Objective Function: The objective function, J, to be minimized, is the net present value (NPV) of the total cost, given as follows:

$$J = J_1 + J_2 + J_3 + J_4. \tag{3}$$

In (3), the microgrid operation cost (MGOC), J_1, is comprised of the cost of unserved demand, generation cost, and start-up/shut-down costs, respectively, given as follows. A 3% annual fuel cost increase (FCI) is assumed:

$$
\begin{aligned}
J_1 = 365 \sum_{i=1}^{G} \sum_{y=1}^{N} \sum_{t=1}^{T} &\left\{ \frac{1}{(1+R)^y} \left[P_{y,t}^{\text{UNS}} \cdot C_{y,t}^{\text{UNS}} \right. \right. \\
&+ (1+\text{FCI})^{y-1} (Pg_{y,i,t}\, b_i + c_i W_{y,i,t}) + \text{SUP}_i U_{y,i,t} \\
&\left. \left. + \text{SDN}_i V_{y,i,t} \right] \right\}.
\end{aligned}
\tag{4}
$$

The BESS installation cost in (3), J_2, is composed of power capacity cost (in $/kW), energy capacity cost (in $/kWh), and a fixed installation cost ($), given as follows:

$$J_2 = \sum_{y=1}^{N} \left[\frac{1}{(1+R)^y} \left(Pb_y^{\text{ini}} C_{pb}^v + E_y^{\text{ini}} C_E^v + B_y C^{fx} \right) \right]. \tag{5}$$

The operating and maintenance (O&M) cost component in (3), J_3, is composed of the fixed and variable O&M costs of the BESS, which vary across technologies and types, given as
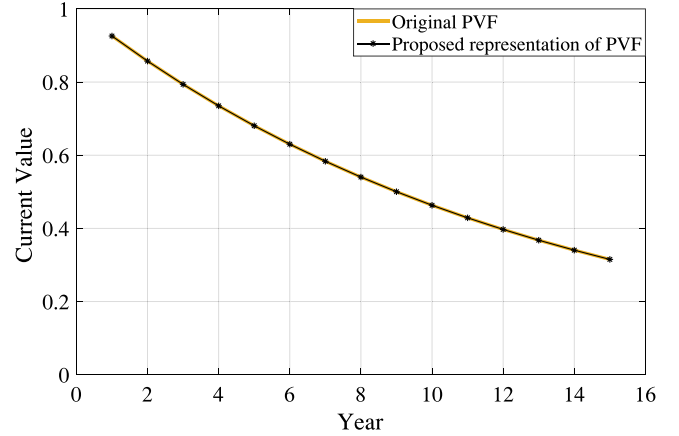

Fig. 2. PVF values over a number of years.

follows:

$$
\begin{aligned}
J_3 = &\underbrace{\sum_{y=1}^{N} \left[\frac{OMC^{fx}}{(1+R)^y} (Pb_y) \right]}_{\text{Fixed O\&M Cost of the Battery}} + \\
&\underbrace{365 \sum_{y=1}^{N} \sum_{t=1}^{T} \left[\frac{OMC^v}{(1+R)^y} \left(\frac{\eta_{\text{ch}}}{1 - \eta_{\text{dch}} \cdot \eta_{\text{ch}}} (-Pba_{y,t}) \right) \right]}_{\text{Variable O\&M Cost of the Battery}}.
\end{aligned}
\tag{6}
$$

The BESS replacement cost in (3), J_4, is included only when the BESS reaches its EoL and has to be replaced, given as follows:

$$J_4 = \left[\frac{1}{(1+R)^{RY}} + \frac{1}{(1+R)^{2RY}} + .. \right] + \varepsilon_y \left(E^{\text{ini}} \text{RC} \right). \tag{7}$$

The replacement year (RY) is initially considered a fixed parameter, as in all studies reported in the literature. When the optimal year of replacement is determined, it is a variable (RY_y^v), and (7) is modified, as the present value factor (PVF) is no longer a constant and is given as:

$$\text{PVF} = \frac{1}{(1+R)^{RY_y^v}} \qquad \forall y. \tag{8}$$

The PVF in (8) is nonlinear, which can be linearized as an infinite series using binomial expression, as follows:

$$\text{PVF} = \left(1 - RY_y^v \cdot R \right) + \frac{(RY_y^v)^2}{2!} - \frac{(RY_y^v)^3}{3!} + \cdots. \tag{9}$$

By replacing the sum of higher order terms of (9) with an equivalent parameter ε_y, which is calculated by subtracting the first term of the binomial expression, $\left(1 - RY_y^v \cdot R \right)$, from the original PVF of (8), a new representation of the PVF can be derived as follows:

$$\text{PVF} = \left(1 - RY_y^v \cdot R \right) + \varepsilon_y \qquad \forall y. \tag{10}$$

It is noted that the PVFs obtained using (9) and the linearized version (10) are exactly matched, as seen in Fig. 2, and hence,

(10) helps avoid the nonlinear terms created by the higher order terms in (9).

The BESS replacement cost, after introducing the replacement year as a variable, is then given as follows:

$$J_4 = \left(1 - R \cdot RY_y^v\right) E_y^{\text{ini}} \text{RC} + \varepsilon_y \left(E_y^{\text{ini}} \cdot \text{RC}\right). \quad (11)$$

2) Model Constraints:

a) Change in the SoC: In order to include BESS degradation, the change in the SoC ($\Delta \text{SOC}_{y,t}$), when the BESS is charging or discharging, is given as follows:

$$\Delta \text{SOC}_{y,t} = \left\{ (\text{SOC}_{y,t+1} - \text{SOC}_{y,t}) \Delta_{y,t}^+ \right\} + \left\{ (\text{SOC}_{y,t+1} - \text{SOC}_{y,t}) \Delta_{y,t}^- \right\} \quad \forall y, t. \quad (12)$$

Equation (12) is linearized to reduce the computational burden. New relations for positive and negative changes in the SoC, $\Delta \text{SOC}_{y,t}^+$, $\Delta \text{SOC}_{y,t}^-$, respectively, are presented as follows:

$$\Delta \text{SOC}_{y,t} = \text{SOC}_{y,t+1} - \text{SOC}_{y,t} \quad \forall y, t \quad (13)$$

$$- M \Delta_{y,t}^- \leq \Delta \text{SOC}_{y,t} \leq M \Delta_{y,t}^+ \quad \forall y, t \quad (14)$$

$$\Delta_{y,t}^+ + \Delta_{y,t}^- \leq \sum_{y=1}^{y=T} B_y \quad \forall y, t \quad (15)$$

$$\sum_{y=1}^{N} B_y = 1 \quad \forall y. \quad (16)$$

Constraint (14) ensures that $\Delta_{y,t}^+$ is unity when $\Delta \text{SOC}_{y,t}$ is positive, and zero otherwise; furthermore, $\Delta_{y,t}^-$ is unity when $\Delta \text{SOC}_{y,t}$ is negative, and zero otherwise. Equation (15) enforces the coordination between $\Delta_{y,t}^+$ and $\Delta_{y,t}^-$, which are binary variables. Equation (16) is a binary constraint for BESS installation and is applied only once during the planning horizon. Furthermore, $\Delta \text{SOC}_{y,t}$ is split into two variables $\Delta \text{SOC}_{y,t}^+$ and $\Delta \text{SOC}_{y,t}^-$, to explicitly calculate BESS degradation due to cycling:

$$-\text{BM} \Delta_{y,t}^- \leq \Delta \text{SOC}_{y,t}^- \leq 0 \quad \forall y \quad (17)$$

$$\Delta \text{SOC}_{y,t}^- \leq \Delta \text{SOC}_{y,t} + (1 - \Delta_{y,t}^-) M \quad \forall y \quad (18)$$

$$\Delta \text{SOC}_{y,t}^- \geq \Delta \text{SOC}_{y,t} - (1 - \Delta_{y,t}^-) M \quad \forall y. \quad (19)$$

Constraint (17) forces $\Delta \text{SOC}_{y,t}^-$ to be equal to zero if $\Delta_{y,t}^-$ is zero, and negative otherwise. The inequality constraints (18) and (19) ensure that $\Delta \text{SOC}_{y,t}^-$ is equal to $\Delta \text{SOC}_{y,t}$ if $\Delta_{y,t}^-$ is unity. The inequality constraints associated with $\Delta \text{SOC}_{y,t}^+$ are similar to (17)–(19), with the exception that $\Delta \text{SOC}_{y,t}^+$ must be positive if $\Delta_{y,t}^+$ is unity, and zero otherwise.

b) BESS sizing with degradation: The BESS energy capacity and year of replacement are determined optimally considering degradation due to calendar, cycling, and number of

C2F, as follows:

$$E_y = \begin{cases} E_y^{\text{ini}} + Edeg_y^{Cyc}, & y = 1 \\ E_{y-1} + Edeg_y^{Cyc} - Edeg_y^{Cal} + AC_y \forall y, & y \neq 1 \end{cases} \quad (20)$$

$$Edeg_y^{Cyc} = 365 \cdot \sum_{t=1}^{24} \left(K \cdot \Delta \text{SOC}_{y,t}^-\right) \quad \forall y \quad (21)$$

$$B_y \leq E_y^{\text{ini}} \leq M \cdot B_y \quad \forall y. \quad (22)$$

Note from (20) that the BESS energy capacity at the year of installation does not consider calendar aging. The capacity lost by degradation during operation is accounted for in (20) by introducing a negative variable $Edeg_y^{Cyc}$. Degradation due to cycling is calculated during discharging in (21), where K is a degradation factor [13] obtained using laboratory measurements. The value of K is chosen as 3×10^{-4} and varies based on BESS technology [13]. Note that the degradation approach in [13] only considers cycling degradation, whereas this work includes both cycling and calendar degradations, as reflected in (20). It should be noted that $Edeg_y^{Cal}$ of the REVBs depends on the Y2D values for each class of EVs.

B_y is a binary variable, taking the value of unity when a BESS is installed at year y, and zero otherwise; the initial BESS energy capacity is assigned optimally using (22).

c) Limit on capital budget of the BESS: This imposes an upper limit on how much capital the microgrid operator can invest in the BESS, over the planning horizon. Accordingly, we have,

$$\sum_{y=1}^{N} \left[\frac{1}{(1 + R)^y} \left(Pb_y^{\text{ini}} C_{pb}^v + E_y^{\text{ini}} C_{pb}^v + B_y C^{fx}\right) \right] \leq \text{BL}. \quad (23)$$

The first and second terms in (23) denote the costs associated with the installed power rating and energy capacity, respectively, and the third term represents the fixed installation cost.

d) Battery energy-to-power ratio constraints: To maintain the energy-to-power ratio $\left(\frac{E}{P}\right)$ of the installed BESS within acceptable limits for the chosen technology, the following constraint is introduced:

$$\underline{\left(\frac{E}{P}\right)} Pb_y \leq E_y \leq Pb_y \overline{\left(\frac{E}{P}\right)} \quad \forall y = 1. \quad (24)$$

e) Standardization of BESS power and energy ratings: The BESS energy and power capacity ratings need to follow available market standards, as follows:

$$E_y^{\text{ini}} = n1_y \cdot \Lambda \quad \& \quad Pb_y^{\text{ini}} = n2_y \cdot \Lambda. \quad (25)$$

It should be noted that $n1_y$ and $n2_y$ are integer variables, and Λ is the standard unit power and energy rating available on the market. In this work, Λ is assumed to be 50 kW.

f) Linearization of battery capacity degradation: As per common practice of BESS manufacturers [14], the battery is warranted to provide desired performance until an SoH of 80% of its rated capacity. Beyond that, the battery is recommended to be replaced, as the manufacturer is no longer responsible for

any malfunction that could occur. In view of the above, the same assumption is used in this work, as follows:

$$\underline{E}_y = 0.8 E^{\text{ini}} \qquad \forall y \qquad (26)$$

$$CRB_y = E_y - \underline{E}_y \qquad \forall y. \qquad (27)$$

E^{ini} is the rated capacity of the BESS; note that (26) imposes the lower limit of BESS capacity before replacement, and if $CRB_y = 0$ or negative in (27), the BESS replacement is due:

$$-M \cdot CF_y^- \le CRB_y \le M \cdot CF_y^+ \qquad \forall y \qquad (28)$$

$$CF_y^+ + CF_y^- \le \sum_{y=1}^{y=T} B_y \qquad \forall y. \qquad (29)$$

Constraint (28) ensures that CF_y^+ is unity when CRB_y is positive, and zero otherwise; similarly, CF_y^- is unity when CRB_y is negative, and zero otherwise. Equation (29) enforces the coordination between CF_y^+ and CF_y^- as:

$$0 \le CRB_y^+ \le M \cdot CF_y^+ \qquad \forall y \qquad (30)$$

$$CRB_y^+ \le CRB_y + (1 - CF_y^+) M \qquad \forall y \qquad (31)$$

$$CRB_y^+ \ge CRB_y - (1 - CF_y^+) M \qquad \forall y. \qquad (32)$$

The inequality constraint (30) states that CRB_y^+ is zero if CF_y^+ is zero, and positive, less than "M" value, otherwise. The inequality constraint (31) ensures that CRB_y^+ is equal to CRB_y if CF_y^+ is unity:

$$-M \cdot CF_y^- \le CRB_y^- \le 0 \qquad \forall y \qquad (33)$$

$$CRB_y^- \le CRB_y + (1 - CF_y^-) M \qquad \forall y \qquad (34)$$

$$CRB_y^- \ge CRB_y - (1 - CF_y^-) M \qquad \forall y. \qquad (35)$$

The inequality constraints (33)–(35) are similar to (30)–(32), with the exception that negative CRB_y^- is considered. The logic-of-status changes, given below, ensure the transitions of states from 0 to 1 when the BESS capacity degrades to the minimum limit; Z_y^{RY} is a binary variable and becomes unity when BESS reaches its year of replacement:

$$Z_{y+1}^{RY} = CF_{y+1}^- - CF_y^- \quad \forall y, y \ne 1 \ : \ Z_y^{RY} = 0; y = 1. \qquad (36)$$

The replacement year is obtained from the following constraint, when Z_y^{RY} is unity:

$$RY_y^v = Z_y^{RY} \times \text{ord}_y \qquad \forall y. \qquad (37)$$

In (37), ord_y is the relative position of each year in the set.

  g) Replacement year bilinear relations: As shown in (11), BESS replacement cost is a bilinear term (product of two continuous variables), not acceptable in mixed-integer programming (MIP) problems. The McCormick method [15] is applied to solve the bilinear term, obtained from multiplication of the two variables RY_y^v and E_y^{ini}, by replacing $\left(RY_y^v \cdot E_y^{\text{ini}} \right)$ with a new variable, LRY_y, which is linked with the two variables, and introducing the inequality constraints (38)–(42). Also, the upper and lower bounds for the two variables of the bilinear

term are chosen appropriately to reduce the search space of the linearized problem (42):

$$LRY_y \ge \underline{E^{\text{ini}}} \, RY_y^v + E_y^{\text{ini}} \, \underline{RY_y^v} - \underline{E^{\text{ini}}} \, \underline{RY_y^v} \qquad \forall y \qquad (38)$$

$$LRY_y \ge \overline{E^{\text{ini}}} \, RY_y^v + E_y^{\text{ini}} \, \overline{RY_y^v} - \overline{E^{\text{ini}}} \, \overline{RY_y^v} \qquad \forall y \qquad (39)$$

$$LRY_y \le \overline{E^{\text{ini}}} \, RY_y^v + E_y^{\text{ini}} \, \underline{RY_y^v} - \overline{E^{\text{ini}}} \, \underline{RY_y^v} \qquad \forall y \qquad (40)$$

$$LRY_y \le \overline{RY_y^v} \, E_y^{\text{ini}} + RY_y^v \, \underline{E_y^{\text{ini}}} - \underline{E^{\text{ini}}} \, \overline{RY_y^v} \qquad \forall y \qquad (41)$$

$$\underline{E^{\text{ini}}} \le E_y^{\text{ini}} \le \overline{E^{\text{ini}}} \quad \& \quad \underline{RY_y^v} \le RY_y^v \le \overline{RY_y^v}. \qquad (42)$$

Finally, the linearized form of (11) is obtained as follows:

$$J_4 = \left(E_y^{\text{ini}} - R \cdot LRY_y \right) \cdot \text{RC} + \varepsilon_y \cdot \left(E_y^{\text{ini}} \cdot \text{RC} \right). \qquad (43)$$

In order to ensure convergence for this linearized model, the constraint relaxation has to be controlled using an appropriate relative optimality gap.

  h) Linearization of BESS replacement year: The BESS energy capacity lost due to degradation, at year y, is given by:

$$LC_y = E^{\text{ini}} - E_y \qquad \forall y. \qquad (44)$$

At the replacement year, the variable AC_y, given below, ensures that the BESS capacity is equal to E^{ini}; accordingly, the various linearized relations are given as:

$$0 \le AC_y \le M \, Z_y^{RY} \qquad \forall y \qquad (45)$$

$$AC_y \ge LC_y + (1 - Z_y^{RY}) M \qquad \forall y \qquad (46)$$

$$AC_y \le LC_y - (1 - Z_y^{RY}) M \qquad \forall y. \qquad (47)$$

  i) BESS power sizing: Note that the BESS power capacity is assumed to remain constant throughout the planning horizon; degradation essentially affects the energy capacity, as follows:

$$Pb_y = \begin{cases} Pb_y^{\text{ini}}, & y = 1 \\ Pb_{y-1} & \forall y, y \ne 1 \end{cases} \qquad (48)$$

$$B_y \le Pb_y^{\text{ini}} \le M \cdot B_y \quad \forall y. \qquad (49)$$

Constraint (49) ensures that BESS power capacity constraints are in effect, once the BESS is installed.

  j) BESS operational constraints: The energy balance of the BESS, where the charging/discharging operations determine the SoC level [16], is given as follows:

$$Pba_{y,t} \cdot \left[\frac{(X_{y,t}^{\text{dch}})}{\eta_{\text{dch}}} + (X_{y,t}^{\text{ch}}) \eta_{\text{ch}} \right] = SOC_{y,t} - SOC_{y,t-1}. \qquad (50)$$

Since the proposed planning problem is solved as an MIP optimization problem, it is essential that (50), which is also nonlinear, is linearized using the "Big-M" method. The linearized equations of charging/discharging constraints can be found in [16]. To force the binary variables associated with the charging and discharging process to be properly activated, several

constraints are used and can found in [16]:

$$-M\, X_{y,t}^{\text{ch}} \leqslant Pba_{y,t} \leqslant M\, X_{y,t}^{\text{dch}} \qquad \forall y, t \qquad (51)$$

$$X_{y,t}^{\text{dch}} + X_{y,t}^{\text{ch}} \leqslant \sum_{y=1}^{N} B_y \qquad \forall y, t. \qquad (52)$$

Constraint (51) ensures that $X_{y,t}^{\text{dch}}$ is unity when discharging, and zero otherwise; it also ensures that $X_{y,t}^{\text{ch}}$ is unity when charging, and zero otherwise. It is assumed that the chosen Li-ion battery has a round-trip efficiency of 90% [17]. The coordination between charging and discharging ensures that decision variables are attained, and that the BESS does not charge and discharge simultaneously, as per (52).

The SoC of the BESS is bound by lower and upper limits; the lower limit depends on the depth of discharge (DoD), as given in the following:

$$E_y \cdot \left(1 - \overline{\text{DoD}}\right) \leqslant SOC_{y,t} \leqslant E_y \qquad \forall y, t. \qquad (53)$$

It should be noted that $SoC_{y,t}$ varies over time and depends on BESS capacity degradation. The maximum allowable DoD of a BESS is denoted by $\overline{\text{DoD}}$.

1) *Charging and discharging operational relations:* In order to capture the O&M cost of the BESS in (3), BESS discharge needs to be calculated accurately. The total energy discharged (TED) is given as follows [8]:

$$TED = \left(\frac{\eta_{\text{ch}}}{1 - \eta_{\text{dch}}\,\eta_{\text{ch}}}\right) \sum_{t=1}^{T} -Pba_{y,t}\, \Delta t \qquad \forall y, t. \qquad (54)$$

2) *Cycling operations constraints:* The maximum number of C2F of the BESS, N_{C2F}, is obtained from the manufacturer as "Wöhler Curve," which captures the effect of BESS cycling degradation on the operations, as follows [7], [8]:

$$365 \cdot \sum_{t=1}^{T} X_{y,t}^{\text{dch}} + X_{y,t}^{\text{ch}} = Cyc_y \qquad \forall t, y \qquad (55)$$

$$\sum_{y=1}^{N} Cyc_y \leqslant N_{\text{C2F}} \qquad \forall y. \qquad (56)$$

Cyc_y is the number of operational cycles of the BESS in year y; the value of N_{C2F} is provided by [17]. Note that Cyc_y can be obtained more accurately by implementing the rainflow algorithm [18], by counting the operation cycles and grouping them in various ranges of DoD, which is beyond the scope of this work.

k) *System operational constraints:* The system demand–supply balance is given as follows:

$$\sum_{i=1}^{G} P_{y,i,t} + Pba_{y,t} + P_{y,t}^{\text{PV}} + P_{y,t}^{W} + P_{y,t}^{\text{UNS}} = (1 + \Gamma)^{y-1} Pd_{y,t}. \qquad (57)$$

Reserve constraints ensure that enough capacity is committed from generators and the BESS to meet the system peak demand

TABLE I
EV PARTICIPANT DATABASE SUMMARY

	Model	Size (kWh)	Datalogging interval
EV1	Ford Focus	23	2013-2016
EV2	Nissan Leaf	24	2013-2016
EV3	Chevrolet Volt	16	2013-2016

TABLE II
NISSAN LEAF VEHICLE (EV2) AND OTHER PARAMETERS

Parameters	Value	Unit	Parameters	Value	Unit
Effective vehicle frontal area (A_f)	2.59	m^2	Air density (ρ)	1.225	(kg/m^3)
Aerodynamic drag coefficient (C_D)	0.28	-	Gearbox ratio (N_g)	7.94	-
Gravitational acceleration (g)	9.81	(m/s^2)	Vehicle mass (m)	1,177	(kg)
Rolling resistance coefficient (C_r)	0.0125	-	Wheel radius (r_w)	0.3	m

and maintain a reserve capacity margin, given as follows [8]:

$$\sum_{i=1}^{G} \left(\overline{Pg_i} W_{y,i,t} - Pg_{y,i,t}\right) + SRB_{y,t} \geq \chi\big[(1 + \Gamma)^{y-1}$$
$$(Pd_{y,t} - P_{y,t}^{\text{UNS}}) + P_{y,t}^{\text{Solar}} + P_{y,t}^{\text{Wind}}\big] \qquad \forall y, t. \qquad (58)$$

In (58), Γ is the annual rate of demand increase and χ is a reserve allocation factor to be maintained taking into account the uncertainty of renewable energy sources.

All standard unit commitment constraints are considered for generating units, such as ramp-up/ramp-down constraints, minimum-up/minimum-down time constraints, and binary coordination constraints, which are discussed in [19].

III. RESULTS AND DISCUSSIONS

A. Input Data, Assumptions, and Test System

1) *Stage I:* In the deterministic case, two realistic drive cycles are considered, FTP-75 and EPA-Highway, emulating an urban-highway-urban round trip of one class of EVs (EV2), presented in Table I, in order to obtain the degradation using the BCDM [20].

On the other hand, for a stochastic case study, three different classes of EV are considered (EV1, EV2, and EV3), with 12 drive cycles for each class of EV, selected based on a *frequency-based feature selection* approach [21]; real-world data are collected and preprocessed, and the drive cycles have been clustered based on EV classes. Table I presents the general data for the three classes of EVs considered in the studies. The EV drive cycle data[1] are based on the actual data collected for three EV classes from the region of Waterloo, ON, Canada, over a period of three years.

The vehicle parameters used to calculate the traction power using VLDM and VPM are presented in Table II for EV2 class [10]. Similar parameters for the other classes of EVs can be found in [22]. It is assumed that the EVB packs for all the EV classes are fully charged at the beginning of the drive cycle,

---

[1] The data were collected in the Drive4Data program, led by the Waterloo Institute for Sustainable Energy. More information is available at: https://wise.uwaterloo.ca/drive4data.

TABLE III
SYSTEM COSTS OF NEW AND REPURPOSED LI-ION BESS

	C_{pb}^v	C_E^v	OMC^{fx}	OMC^v	RC	Energy-Unit	Power-Unit
	$/kW	$/kWh	$/kWh	$/kWh	$/kWh	$/kWh	$/kW
New	1,859	901	13.2	0.0014	1,560	445	525
Re-purposed	1,334	456	13.2	0.0018	1,115	200	236

Fig. 4. PV and wind hourly generation profiles.
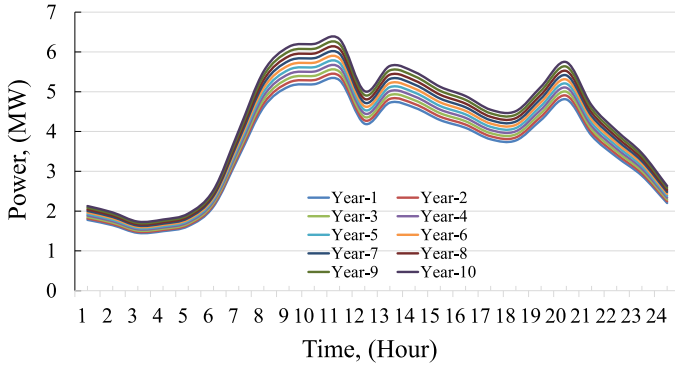
Fig. 3. Isolated microgrid hourly demand profile of each year ($Pd_{y,t}$).

Fig. 5. (a) EVB normalized capacity for one-day driving. (b) EVB normalized capacity for seven-year driving.

and their SoC is allowed to vary between 20% and 90% during operation.

It should be noted that the battery type of all EV classes is Li-ion pack as per information given by their manufactures.

2) Stages II and III: The Li-ion battery is considered for both new and repurposed BESSs, whose costs are given in Table III. The microgrid has a total investment budget of $2.5 million. The maximum DoD is assumed to be 80%, whereas the $\frac{E}{P}$ ratio is between 1 and 4 [17]. The energy cost of REVBs is obtained in Stage II, which is multiplied by different factors obtained from [17] to estimate the different cost components of an REVB system. Note that the cost of installing an REVB as a BESS is the same as installing a new BESS.

The proposed BESS planning model is validated and tested on the CIGRE isolated microgrid benchmark system [23], which features the following components: three diesel units with ratings of 2,500 kW (DG1), 1,400 kW (DG2), and 800 kW (DG3); a 310-kW CHP-diesel unit (DG4); a 500-kW gas microturbine (DG5); and eight photovoltaic (PV) units and four wind turbine units, with total installed capacities of 840 and 1,450 kW, respectively [23]. These dispatchable and nondispatchable units supply the peak demand of 5.29 MW in the first year, which increases annually at the rate 2% over a ten-year planning horizon [23]. The proposed BESS sizing model is executed on forecasted profiles of average power demand and solar and wind generation, shown in Figs. 3 and 4 [23]. The operating reserve requirement of the isolated microgrid is 13% of the hourly demand. The fixed installation cost is $ 20,000, which is incurred only once. When the replacement year of the BESS is assumed to be fixed, the BESS is replaced every five years. The discount rate (R) of the planning problem is assumed to be 8%, and the maximum BESS energy capacity and power rating that can be installed are 10 MWh and 10 MW, respectively. It should be
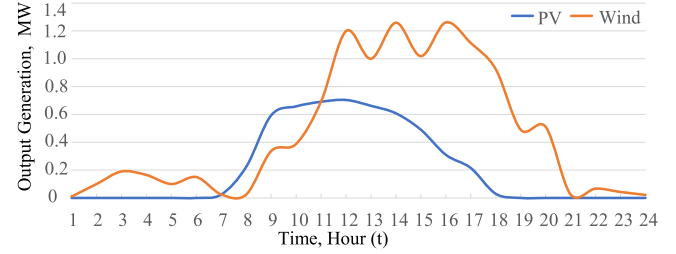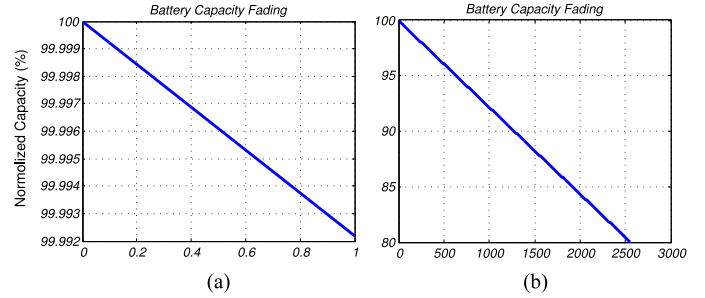
noted that the Big-M value is set to be 10,000 which is similar to the maximum BESS energy capacity.

B. Results and Analysis

1) Stage I:

a) Deterministic case study: The Stage I models are solved for a realistic urban–highway–urban round trip drive cycle, which results in degradation of the EVB pack to an SoH of 80.2% of the original capacity of 24 kWh (EV2 class), with $\zeta = 4.752$ kWh. The degraded capacity after one-daily drive cycle is 0.00775% of the initial capacity [see Fig. 5(a)], and it is noted that the EVB reaches an SoH of 80.2% after seven years on the road [see Fig. 5(b)]. Assuming that the EVBs have a calendar life of 15 years [24], seven years on the road means that they have a remaining calendar life of eight years.

b) Stochastic case study: First, each EV class of parameters described in Table I and their 12-selected drive cycles were simulated. The number of driving cycles found to reach the threshold of SoH (80%) is then determined. Fig. 6(a)–(c) shows the number of driving cycles required by each class of EV to reach an SoH of 80%. Each EVB reaches its 80% SoH depending on how harsh the acceleration and braking events were for that vehicle's drive cycle. Since each drive cycle represents a one-day driving operation, the number of years that it takes for the EVB to degrade to an SoH of 80%, denoted by Y2D, can be calculated as follows:

$$\text{Y2D} = \text{Number of drive cycles to 80\% SoH}/365. \quad (59)$$

After determining the Y2D of each drive cycle, it is then multiplied by a uniform probability distribution function to determine the expected Y2D, denoted by E(Y2D), for each EV class,
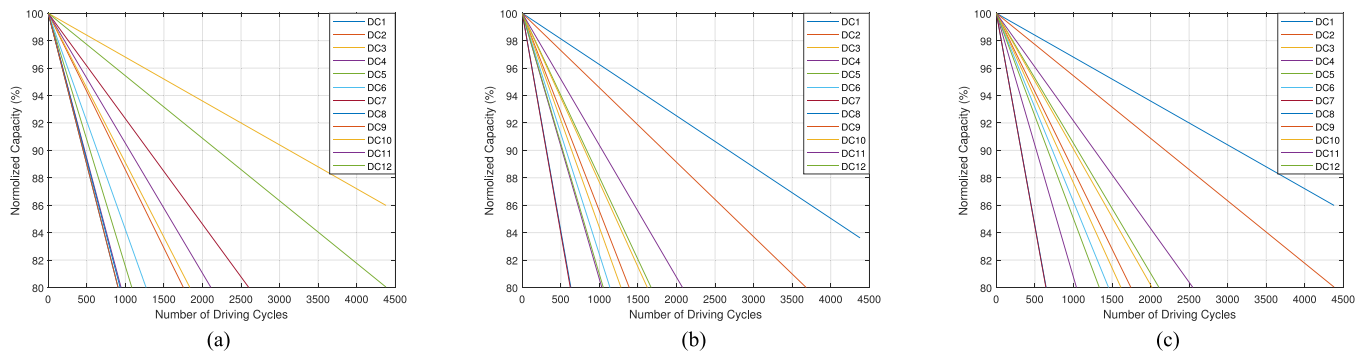
Fig. 6. EVB normalized capacity for different drive cycles and EV classes. (a) EV1. (b) EV2. (c) EV3.

which will impact Stages II and III. The remaining life of an EVB will impact the cost of REVBs and later will influence their replacement year in the microgrid planning model. For the drive cycles considered in this work, it is noted that the value of E(Y2D) is 5.6 years for class EV1, 5.1 years for class EV2 is, and 5 years for class EV3. These values are less than those in the deterministic case because of the presence of numerous real data scenarios of the drive cycles. Accordingly, there would be early replacements for EVBs during their first-life and longer calendar years for REVBs in microgrid applications.

The stochastic studies demonstrate how to capture and represent the heterogeneity of REVBs in the real world (e.g., different charging/discharging coefficients, different remaining capacities for second-life purpose in microgrids, and different characteristics) by clustering and integrating within the proposed planning model.

Thus, modeling the performance of the EVB on the road over a number of years until it reaches its 80% SoH provides the inputs needed for Stage II. It should be noted that varying drive cycles, initial SoC, and other parameters of an EVB would result in a different SoH and, in turn, a different REVB cost, as presented in the stochastic case.

2) Stages II and III: The outputs of Stage I of the deterministic case are introduced as inputs to Stage II; the results show that the cost of the used Li-ion EVB of 80.2% SoH is 141 $/kWh, and the effective repurposing cost is 59 $/kWh. The total cost of the REVB is, therefore, 200 $/kWh. These values are compared with those for a new Li-ion BESS (see Table III) and introduced as inputs to Stage III. It should be noted that the REVB cost is based on the EV2 class of the Nissan Leaf battery with a capacity of 24 kWh. In order to examine the suitability of the proposed BESS planning model, the following cases are considered.

1) Base Case: no BESS installation;
2) Case I: with an REVB as a BESS;
3) Case II: with a new BESS.

For Cases I and II, the following four scenarios pertaining to the BESS are studied:

a) Fixed year of replacement, no degradation;
b) Fixed year of replacement, considering degradation;
c) Variable replacement year, considering degradation;
d) Variable replacement year, considering degradation, with no C2F constraints.

The microgrid operator has the option to install the BESS, either new or REVB, with the objective of lowering the total NPV of costs, and thereby increasing its participation in the system reserve service provisions and discharging energy during peak periods. Also, the microgrid operator will optimally replace the BESS based on the introduced set of constraints to avoid premature replacement and additional costs. As shown in Table IV, for Case I, Scenario *a*, the total cost of the microgrid is $60,501,295, which is considerably lower than that without the BESS (Base Case), when the cost is $82,097,474. The size of the BESS as an REVB is optimally determined in Case I, Scenario *a*, to be 800 kWh with power rating of 600 kW; since the degradation effect is not taken into account, the BESS size is determined based on the terminal year requirements, which implicitly satisfies previous year requirements as well. The operation of the microgrid for one day in year 5 of Case I, Scenario *a*, is highlighted in Fig. 7, which presents the supply–demand balance, where the supply is represented by stacked areas including two discharging events of REVBs and the total load of the microgrid is represented by a solid line.

In Case I, Scenario *b*, which considers BESS calendar and cycling degradations, a 1,050-kWh/600-kW REVB is optimally determined for the BESS in the microgrid. Even though the total microgrid cost is increased, the incremental cost of $869,137 (compared to Case I, Scenario *a*) captures the BESS size accurately. The optimal scheduling and planning decisions indicate that the cost of isolated microgrid operation is higher when BESS degradation is considered, since the operation is more accurately modeled, and the microgrid operator adjusts the energy allocation (reserve and discharging) of BESS accordingly. It should be noted that degradation due to cycling is only counted during discharging. Considering a flat rate of cycling degradation would lead to premature replacement, and additional costs (overestimating BESS sizes) would be incurred, since each system operator has different operating characteristics. However, when considering both cycling and calendar degradations accurately, the sizes would be obtained, and premature replacements are prevented.

Case 1, Scenario *c*, considers both the optimal year of replacement and the impact of degradation, the total cost of the microgrid is reduced, and a saving of $806,800 is achieved, as compared to Case I, Scenario *b*. Although the size of the REVB is greater than that in Case I, Scenario *b*, of 1,200 kWh/650 kW,

TABLE IV
OPTIMAL BATTERY SIZING SOLUTIONS

	Base Case	Case I: with REVBs				Case II: with New BESS			
Scenario-	-	a	b	c	d	a	b	c	d
Deg./RY.*	-	No/ Fixed	Yes/ Fixed	Yes/Variable	Yes/Variable	No/ Fixed	Yes/ Fixed	Yes/Variable	Yes/Variable
J, $	82,097,474	60,501,295	61,370,432	60,563,632	60,371,250	61,534,080	62,556,243	61,885,146	61,873,402
J_1, $	82,097,474	58,329,594	58,774,730	59,235,576	57,756,013	58,465,019	58,927,916	59,746,674	58,155,742
J_2, $	-	1,097,407	1,202,963	1,328,056	1,640,000	1,676,991	1,799,491	2,138,472	2,433,102
J_3, $	-	54,045	53,663	58,095	71,638	53,852	49,078	58,049	62,469
J_4, $	-	1,020,249	1,339,077	780,710	903,600	1,338,219	1,779,758	1,179,678	1,222,088
RY_y [year]	-	every 5 years		7	8	every 5 years		6	8
Pb_y [kW]	-	600	600	650	800	600	550	650	700
E_y [kWh]	-	800	1,050	1,200	1,500	750	950	1,200	1,450

* Deg./RY. denotes degradation and replacement year, respectively, if they considered.

the optimal replacement year, which is year 7, ensures that the premature replacement observed in other scenarios is prevented. The replacement cost in Case I, Scenario c, is decreased by $558,366, as the year of replacement is deferred to the seventh year, as against that in Scenarios a and b of Case I, and most of the work reported in the literature, where replacement year is fixed, results in inaccurate BESS planning decisions. Moreover, implementing the optimal year of replacement prevents more replacements over the planning horizon, which reduces capital expenditure. If degradation and optimal replacement year are ignored, the model's optimal decisions will be affected and, hence, reflected on the total cost of the microgrid, as well as its reliability during operation.

It is noted that in all Scenarios of Case II (see Table IV), installing a new BESS increases the microgrid total cost. Comparing Case I, Scenario c, with Case II, Scenario c, it is seen that the microgrid achieves a saving of $ 1,321,514 over the planning horizon when an REVB is installed as the BESS instead of a new BESS. However, it should be noted that the battery management system (BMS) of the REVB has to be as reliable as a new BESS. As in Case I, Scenario c, when the model considers optimal replacement year in Case II, Scenario c, a significant cost saving of $671,097 compared to Case II, Scenario b, is achieved over the ten-year planning horizon.

Table IV also shows that optimal investments in REVBs significantly reduces the microgrid cost over the planning horizon. The optimal planning model leads to further superior results after the replacement year is made a variable. When the replacement year was fixed, the system accrued additional costs, since the BESS had not reached its EoL at the year of replacement. This premature replacement added more cost to the microgrid operator, as seen in Scenario b of Cases I and II.

Similarly, when the optimal planning model does not consider BESS degradation (*Scenario a in Cases I and II*), the total cost of the microgrid, (J), is the lowest among the scenarios pertaining to that case, and it does not reflect the true cost of the microgrid. Optimal year of BESS replacement in scenario c in Cases I and II occurs when the battery capacity reaches 80% of its original rated capacity. Accordingly, in Table IV, Case I, Scenario c, shows that the BESS is optimally replaced in year 7, while Case II, Scenario c, shows that the BESS is optimally replaced in year 6, and not in year 5 as in Scenarios a and b of Cases I and II.
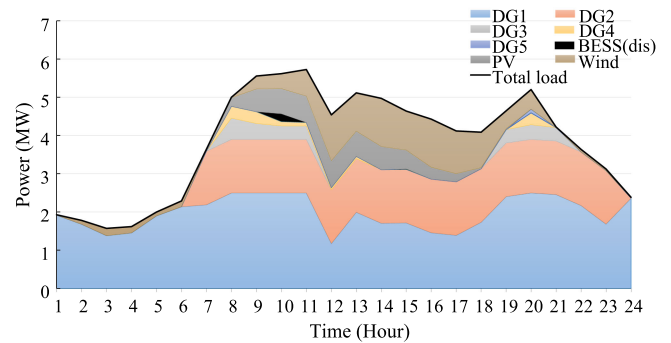

Fig. 7. Supply and demand mix in year 5 of Case I, Scenario a.

The impact of BESS capacity degradation due to cycling and calendar aging is fully considered, given that the BESS degrades when there is a discharging process. Most of the BESS sizing problems found in the literature consider a fixed degradation during cycling at each year irrespective of the operation, thereby obtaining a size and cost that are not quite accurate. When no degradation is considered, as in Scenario a, the sizing of the REVB is lower than that when the degradation model is implemented. The lower sizing is optimally chosen because the model sizes the REVB at the terminal year when the load is the highest, assuming that the REVB energy size will not degrade with time. This consideration is not valid even though it has the least cost among all Scenarios.

The optimal replacement year would be most important when considering the distributed BESS. Since each BESS operation would be different, the replacement year will also be different.

Most energy management and resource allocation studies for BESS sizing do not explicitly consider life-cycle degradation due to C2F or discharging. The latter leads to BESS size degradation, which has a great impact on the operation of a system. In these cases studies, since REVBs have a lower number of C2F as compared to new BESSs, the microgrid operator tends to allocate more reserves to the REVBs instead of discharging them, while the new BESSs are scheduled for discharging operations much more. This is shown in Fig. 8, which compares between the reserve allocated to REVBs *vis-à-vis* new BESSs. More discharging, understandably, leads to earlier replacement year for new BESSs as compared to REVBs.
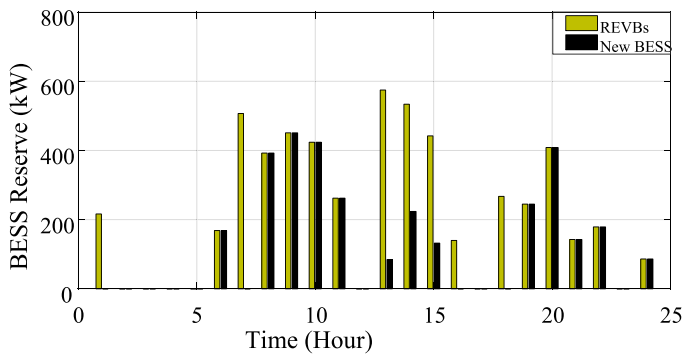
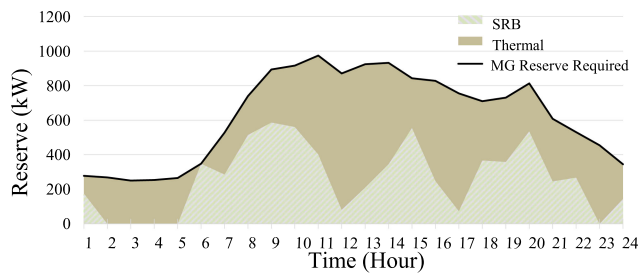Fig. 8. Reserves allocation of new BESSs and REVBs in year 9 of Scenario a of Cases I and II.

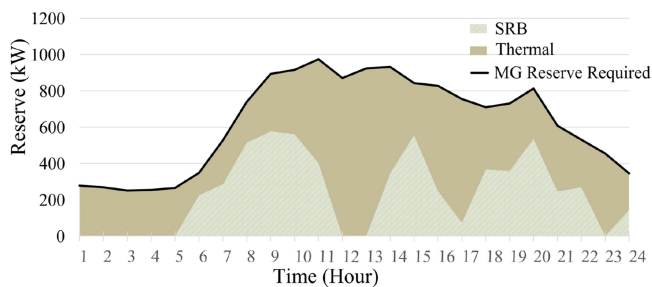Fig. 9. Reserve provisions in year 10 of Case I, Scenario c.

Fig. 10. Reserve provisions in year 10 of Case II, Scenario c.

Fig. 11. Average reserve over planning horizon.
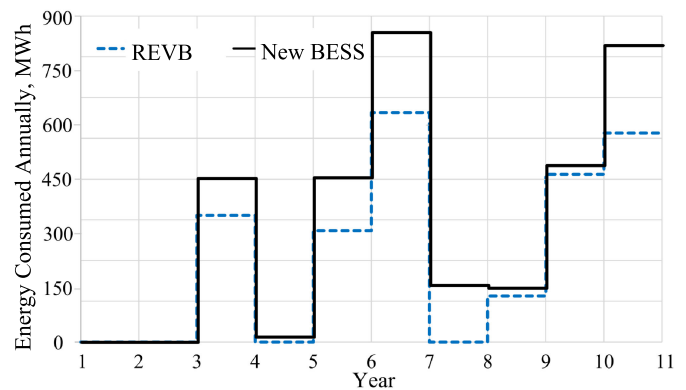
Fig. 12. Annual energy consumption over planning horizon.

Allocating more reserves is reflected as well, in the optimal replacement year to be year 7, in Case I, Scenario c, as against year 6 in Case II, Scenario c, as shown in Table IV. However, in Case II, the microgrid operator tends to discharge more energy, since a new BESS has a higher number of C2F. Figs. 9 and 10 depict the total microgrid reserve allocated by the microgrid operator in year 10 to the thermal generators, REVBs, and new BESSs to meet the reserve requirements.

It is noted from Fig. 11 that the average reserve allocation is mostly higher for REVBs as compared to new BESSs. Also, it is clear from Fig. 12 that new BESS units are involved more in energy buffering than REVBs. In the first and second years, both new BESSs and REVBs are assigned only for reserve allocation so that the battery does not degrade while buffering. Also, the REVB is assigned for reserve allocation only, in years 4 and 7, since it has fewer C2F as compared to new BESS.

In Scenario d of Cases I and II presented in Table IV, the C2F constraints are not considered. Due to the fact that the BESS does not have li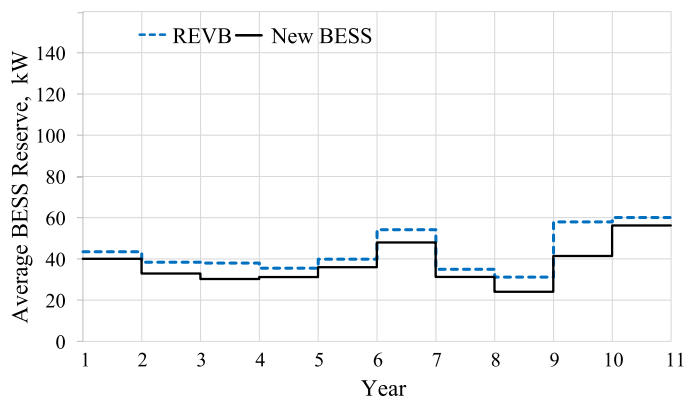mits on C2F, the BESS tends to discharge more, which results in more degradation of the battery, that necessitates the system to have a larger size of the BESS. Also, the replacement year of the BESS is shifted to a later year. Even though the total MGOC is reduced, this reduction does not reflect the true operation cost of the microgrid. Case I, Scenario d, demonstrates how the replacement year of REVBs is limited by the calendar degradation and REVBs have to be replaced in year 8, which is affected by Stage I outputs, and demonstrates why it is important to consider Stage I.

3) Stochastic Case Study of Stages II and III: After the REVBs are clustered into three classes, the optimal decisions for different classes are obtained separately. The results obtained for each class are presented in Table V; only Scenario c of Case I is considered. It is evident that the results of all the EV classes are quite similar. The installed REVB system based on the EV1 class has a higher operation and planning cost than EV2 or EV3 because it has a higher Y2D, which was obtained in Stage I, and a lower number of C2F. EV2 and EV3 yield the same optimal solutions because they have quite similar values of Y2D and C2F.

IV. ALGORITHMS AND COMPUTATIONAL ASPECTS

The Stage I models—VLDM, VPM, and BCDM—are programmed and simulated in MATLAB/Simulink. The proposed microgrid planning model is programmed and executed in the GAMS environment on an IBM Server xSeries 460 with eight Intel Xeon 2.8-GHz processors and 3 GB (effective) of RAM.

TABLE V
OPTIMAL SOLUTIONS WITH DIFFERENT EV CLASSES

	Case I Scenario C: with REVBs	
EV Class	**EV1**	**EV2 and EV3**
Deg./RY.*	**Yes/ Variable**	**Yes/ Variable**
J, \$	**60,339,949**	**60,171,400**
J_1, \$	58,172,088	58,000,046
J_2, \$	1,328,056	1,328,056
J_3, \$	59,095	62,588
J_4, \$	780,710	780,710
RY_y [year]	7	7
Pb_y [kW]	650	650
E_y [kWh]	1,200	1,200

*Deg./RY. denotes degradation and replacement year, respectively, if they considered.

TABLE VI
MODEL STATISTICS

	Base Case	Case I(c)
Model Type	MILP	MILP
Solver Used	CPLEX	CPLEX
Number of Single Equations	5,541	12,434
Number of Single Variables	5,581	8,373
CPU time	0.182 (s)*	4 (h)*

*(s) and (h) denote second and hour, receptively.

The optimization model is a mixed-integer linear programming (MILP) model, which is solved using the CPLEX solver, which provides an option to use either Benders decomposition algorithm, or by default, uses the conventional branch and bound (B&B) algorithm. In this work, the CPLEX was set to use the default B&B algorithm [25]. The MILP optimal solution is obtained by setting the optimality gap to 5%. The model and solver statistics for the chosen cases are given in Table VI.

The average computational time for the optimization problem of Stage III is about 3.5 h for all the cases and Scenarios, except the Base Case.

A. Comments on Linearization

In mathematical programming, the concept of linearization involves approximating a given function using a linear function in an interval. In this work, three different linearization methods are used for different tasks. First, the PVF of (8) is linearized as an infinite series using a binomial expression. By replacing the sum of higher order terms of (9) with ε_y, a new representation of the PVF is derived. This linearization is only a transformation and does not impact the accuracy, as shown in Fig. 2. The second type of linearization involves linearizing the product of a binary and a continuous variable, and is used at multiple instances, in the BESS operational and sizing constraints. This linearization uses the commonly used Big-M method, where an additional set of linear constraints is used to represent the product of two variables. The linear set of constraints are effectively modeled to represent the product of variables in an exact form. There is no approximation and, hence, no loss of accuracy. The third type of linearization is McCormick linearization [15], which is used to

TABLE VII
BOUNDARY LIMITS OF NONLINEAR VARIABLES

	Lower Limits	Upper Limits
RY_y^v	1 year (new BESS)	10 years
RY_y^v	1 year (REVBs)	Depends on Y2D
E_y^{ini}	0 MWh	10 MWh

linearize the term associated with the replacement cost J_4 in (7). McCormick linearization is a convex relaxation approach used for bilinear variables (product of two continuous variables), wherein the lower and upper bounds of the two continuous variables are chosen in such a way that the search for the optimal solution is within practical limits of computation. It should be noted that the chosen boundaries of the two variables define the solution space.

In this work, the variables of concern in J_4 (7) are the replacement year (RY_y^v) and the BESS capacity (E_y^{ini}). As noted from Table VII, the lower and upper bounds of these variables are chosen based on realistic considerations of the microgrid planner; for example, the maximum BESS capacity to be installed is chosen to be 10 MWh, which is governed by external factors such as budgetary limits or policy decisions. The replacement year for REVBs depends on the remaining life of the batteries. It should be noted that the accuracy of the planning model will not be impacted by the process of linearization.

V. CONCLUSION

The large-scale deployment of BESSs within microgrids is constrained by their high investment cost barrier, while the availability of used EVBs has created a less expensive option for the planners. Researchers have, thus far, not taken into account BESS degradation, in sizing and life-cycle assessment for microgrid long-term planning models. This paper develops a systematic procedure to model the degradation of EVBs for different classes of EV during their first-life. This model is integrated into a novel microgrid planning model that determines the optimal decisions of new BESS and REVBs and their corresponding sizing and year of installation, taking into account a new set of mathematical relations of BESS degradation and optimal year of replacement. REVBs are modeled considering their first-life drive cycles and degradation models, which impacts the microgrid planning decisions, if not considered. Stages I and II of the proposed framework quantify the EV battery first-life and a process to calculate the cost of REVB. The model in Stage I can be used by researchers and EV manufacturers to develop a dataset of EV batteries pertaining to their life. The mathematical model in Stage III of the proposed framework is targeted to a microgrid or a distribution system planner, wherein the planner accesses the dataset from Stages I and II, for the model in Stage III. To have a robust operation of REVBs, they are assumed to be equipped with a BMS that controls the output of the REVBs. Further work is needed to ease the computational burden and to adopt more dynamic decision variables for which decomposition methods are appealing options.

REFERENCES

[1] IEA, "Outlook 2017: Two million and counting," 2017. [Online]. Available: https://www.iea.org/publications/freepublications/publication/GlobalEVO utlook2017.pdf

[2] CNET, ABB & GM, Jun. 2017. [Online]. Available: http://www.cnet.com/uk/news/nissan-leafbatteries-seek-second-life-as-ho me-storage

[3] J. Neubauer, K. Smith, E. Wood, and A. Pesaran, "Identifying and overcoming critical barriers to widespread second use of PEV batteries," Nat. Renew. Energy Lab., Golden, CO, USA, Tech. Rep. NREL/TP-5400-63332, 2015.

[4] E. Cready, J. Lippert, J. Pihl, I. Weinstock, and P. Symons, "Technical and economic feasibility of applying used EV batteries in stationary applications," Sandia Nat. Lab., Albuquerque, NM, USA, Tech. Rep. SAND2002-4084, 2003.

[5] L. Lam and P. Bauer, "Practical capacity fading model for li-ion battery cells in electric vehicles," *IEEE Trans. Power Electron.*, vol. 28, no. 12, pp. 5910–5918, Dec. 2013.

[6] K. Baker, G. Hug, and X. Li, "Energy storage sizing taking into account forecast uncertainties and receding horizon operation," *IEEE Trans. Sustain. Energy*, vol. 8, no. 1, pp. 331–340, Jan. 2017.

[7] I. Alsaidan, A. Khodaei, and W. Gao, "A comprehensive battery energy storage optimal sizing model for microgrid applications," *IEEE Trans. Power Syst.*, vol. 33, no. 4, pp. 3968–3980, Jul. 2018.

[8] H. Alharbi and K. Bhattacharya, "Stochastic optimal planning of battery energy storage systems for isolated microgrids," *IEEE Trans. Sustain. Energy*, vol. 9, no. 1, pp. 211–227, Jan. 2018.

[9] S. Saxena, C. L. Floch, J. MacDonald, and S. Moura, "Quantifying EV battery end-of-life through analysis of travel needs with vehicle powertrain models," *J. Power Sources*, vol. 282, pp. 265–276, 2015. [Online]. Available: http://www.sciencedirect.com/science/article/pii/S0378775315000841

[10] A. Ostadi and M. Kazerani, "Optimal sizing of the battery unit in a plug-in electric vehicle," *IEEE Trans. Veh. Technol.*, vol. 63, no. 7, pp. 3077–3084, Sep. 2014.

[11] X. Lin *et al.*, "Online parameterization of lumped thermal dynamics in cylindrical lithium ion batteries for core temperature estimation and health monitoring," *IEEE Trans. Control Syst. Technol.*, vol. 21, no. 5, pp. 1745–1755, Sep. 2013.

[12] National Renewable Energy Laboratory, *NREL Battery Second-Use Repurposing Cost Calculator for Electric Vehicles*, 2018. [Online]. Available: https://www.nrel.gov/transportation/b2u-calculator.html, 2018.

[13] Y. Riffonneau, S. Bacha, F. Barruel, and S. Ploix, "Optimal power flow management for grid connected PV systems with batteries," *IEEE Trans. Sustain. Energy*, vol. 2, no. 3, pp. 309–320, Jul. 2011.

[14] E. M. Krieger, J. Cannarella, and C. B. Arnold, "A comparison of lead-acid and lithium-based battery behavior and capacity fade in off-grid renewable charging applications," *Energy*, vol. 60, pp. 492–500, 2013. [Online]. Available: http://www.sciencedirect.com/science/article/pii/S0360544213007044

[15] P. M. Castro, "Tightening piecewise McCormick relaxations for bilinear problems," *Comput. Chem. Eng.*, vol. 72, pp. 300–311, 2015.

[16] F. Ramos, C. Cañizares, and K. Bhattacharya, "Effect of price responsive demand on the operation of microgrids," in *Proc. Power Syst. Comput. Conf.*, Aug. 2014, pp. 1–7.

[17] A. A. Akhil *et al.*, *DOE/EPRI 2013 Electricity Storage Handbook in Collaboration With NRECA*. Albuquerque, NM, USA: Sandia Nat. Lab., 2013.

[18] S. Downing and D. Socie, "Simple rainflow counting algorithms," *Int. J. Fatigue*, vol. 4, no. 1, pp. 31–40, 1982.

[19] M. Carrion and J. M. Arroyo, "A computationally efficient mixed-integer linear formulation for the thermal unit commitment problem," *IEEE Trans. Power Syst.*, vol. 21, no. 3, pp. 1371–1378, Aug. 2006.

[20] United States Environmental Protection Agency (EPA), "Vehicle and Fuel Emissions Testing," 2017. [Online]. Available: https://www.epa.gov/vehicle-and-fuel-emissions-testing/dynamometer-drive-schedules

[21] C. Robert and G. Casella, *Monte Carlo Statistical Methods*. New York, NY, USA: Springer, 2013.

[22] M. Ehsani, Y. Gao, and A. Emadi, *Modern Electric, Hybrid Electric, and Fuel Cell Vehicles: Fundamentals, Theory, and Design*. Boca Raton, FL, USA: CRC Press, 2009.

[23] D. E. Olivares, C. A. Cañizares, and M. Kazerani, "A centralized energy management system for isolated microgrids," *IEEE Trans. Smart Grid*, vol. 5, no. 4, pp. 1864–1875, Jul. 2014.

[24] USCAR, "*FreedomCAR and USABC energy storage goals for power-assist HEVs*," 2002. [Online]. Available: http://www.uscar.org/commands/files_download.php?files_id=83

[25] GAMS Development Corporation, General Algebraic Modeling System (GAMS), software, 2017. [Online]. Available: http://www.gams.com

Talal Alharbi (S'13) received the B.Sc. degree in electrical engineering from Qassim University, Buraydah, Saudi Arabia, in 2010, and the M.A.Sc. degree in electrical and computer engineering in 2015 from the University of Waterloo, Waterloo, ON, Canada, where he is currently working toward the Ph.D. degree with the Department of Electrical and Computer Engineering.

He is also a Lecturer with the Department of Electrical Engineering, Qassim University. His research interests include power system operations, power electronics, microgrids, and smart grids.

Mr. Alharbi received the Best Paper Award from the 15th Annual IEEE Canada Electrical Power and Energy Conference in 2015.

Kankar Bhattacharya (M'95–SM'01–F'17) received the Ph.D. degree in electrical engineering from the Indian Institute of Technology, New Delhi, India, in 1993.

He was with the faculty of the Indira Gandhi Institute of Development Research, Mumbai, India, during 1993–1998 and, then, with the Department of Electric Power Engineering, Chalmers University of Technology, Gothenburg, Sweden, during 1998–2002. In 2003, he joined the Department of Electrical and Computer Engineering, University of Waterloo, Waterloo, ON, Canada, where he is currently a Full Professor. His research interests include power system economics and operational aspects.

Mehrdad Kazerani (M'96–SM'02) received the B.Sc. degree from Shiraz University, Iran, in 1980, the master's degree from Concordia University, Montreal, QC, Canada, in 1990, and the Ph.D. degree from McGill University, Montreal, in 1995.

From 1982 to 1987, he was with the Energy Ministry of Iran. He is currently a Professor with the Department of Electrical and Computer Engineering, University of Waterloo, Waterloo, ON, Canada. His research interests include power electronics, power quality, distributed power generation, utility interface of alternative energy sources, battery electric, hybrid electric and fuel cell vehicles, and flexible ac transmission systems.

Dr. Kazerani is a registered Professional Engineer in the province of Ontario, Canada.